Hadley Cell Expansion and Extratropical Drying Over Land

Daniel Flint Schmidt

Lynchburg, Virginia

B.S. Mathematics, Liberty University, 2007

M.S. Mathematics, Virginia Tech, 2010

Ph.D. Mathematics, Virginia Tech 2015

A Thesis presented to the Graduate Faculty of the University of Virginia in Candidacy for the Degree of Master of Science

Department of Environmental Sciences

University of Virginia

August, 2018

Abstract

Numerous lines of observational evidence suggest that Earth's tropical belt has expanded over the past 30–40 years. It is natural to expect that this poleward displacement should be associated with drying on the poleward margins of the subtropical dry zones. However, such drying may be heavily modified by other processes, and may be zonally asymmetric. This study tests the degree to which poleward motion of the Hadley cell boundary is associated with changes in local precipitation or sea level pressure, and the degree to which those changes are zonally symmetric. Evidence from both reanalysis data and global climate models reveals that the local changes associated with Hadley cell expansion are mostly confined to certain centers of action which lie primarily over oceans. Consequently, the tropical expansion measured by zonally averaged variables is not associated with systematic drying over subtropical land regions, as is often assumed.

1. Introduction

1.1 The Hadley Cells

Earth's climate at low latitudes is dominated by meridional overturning circulations known as Hadley cells. In the annual mean, the processes driving these cells can be described as follows. Near the thermal equator, intense convection occurring in thunderstorms carries air from the surface to the upper troposphere. Due to the static stability of the stratosphere, the air is unable to rise farther, so it spreads poleward in both the Northern and Southern Hemispheres, turning eastward due to the Coriolis effect and driving the subtropical jet streams. This upper tropospheric air eventually cools radiatively and sinks around 30 degrees latitude in each hemisphere. A return flow near the surface brings air back toward the Equator, turning toward the west as it does so and creating northeasterly trade winds in the Northern Hemisphere and southeasterly trade winds in the Southern Hemisphere.

The Hadley circulation described above is essentially a heat engine, and its physics is most easily explained in terms of the transport of *moist static energy,* defined as the sum of gravitational potential energy, latent heat, and sensible heat:

$$S = gz + L_v q + c_P T$$

Here g is the acceleration of gravity, z is the geopotential height, L_v is the latent heat of vaporization of water, q is the specific humidity of the air, c_P is the specific heat capacity of air at constant pressure, and T is the absolute temperature. Note that moist static energy, as defined here, is actually energy per unit mass, so that it will have units of m^2/s^2 or J/kg, rather than simply Joules. A related variable is equivalent potential temperature, denoted θ_e, which represents the temperature that an air parcel would have if all of its water vapor condensed out (converting the latent heat to sensible heat) and if it was brought to a reference level arbitrarily fixed at 1000 hPa (converting the gravitational potential energy to sensible heat). Moist static energy and equivalent potential temperature are essentially interchangeable, in the sense that any process that conserves one will conserve the other.

The Hadley cells exist due to the meridional distribution of net radiation, which is positive in the tropics and negative in the polar regions, producing a surplus of energy in the tropical regions, which must be transported poleward to balance the deficit of energy at higher latitudes. The surplus of radiant energy at the tropical surface is transferred to the overlying air in the form of both sensible and latent heat, and thus air in the lower part of the rising branch is both warm and humid. As the air rises, it cools at the moist adiabatic lapse rate, losing much of its water vapor content. During this ascent the latent heat and sensible heat are transformed to gravitational potential energy, but total moist static energy is approximately conserved. As the air moves poleward at high altitudes, however, it cools by thermal infrared emission to space, and does in fact lose energy. When the air eventually sinks at higher latitudes, it warms at the dry adiabatic lapse rate. Since the dry adiabatic lapse rate is much larger than the moist adiabatic lapse rate, the air warm in the descent more than it cooled on the ascent. This counteracts the loss of heat to space, meaning that the descending air eventually returns to nearly the same temperature as at the thermal equator. However, the air is by this time very dry, and thus has low moist static energy. The energy is replaced by evaporation of water into the air as the air returns toward the equator on the trade winds.

Thus, the Hadley cells are driven by the positive flux of net radiation at the tropical surface, and their net effect is to transport the resulting energy both upward and poleward to regions where the net radiative flux is negative. Such a “thermally direct” circulation could occur even in a dry atmosphere (as it does on Venus). In this case, ascent and descent would both be relatively slow, and would occur over approximately equal areas. In a moist atmosphere, however, the Hadley cells also have the effect of transporting water vapor equatorward. Consequently, the effect of moist processes at the equator is to enhance convection, concentrating the resulting rapid ascent in a narrow band, while the descent occurs more slowly over a broader area (James, 1994, pp. 98-99). This distinction is important. While a dry atmosphere could sustain a meridional overturning circulation, it would need to have a very different temperature profile. Earth’s actual atmosphere is

on average absolutely stable above 600 hPa in the tropics. (That is, the environmental lapse rate is slightly smaller than the moist adiabatic lapse rate, or equivalently, θ_e increases with altitude.) Large-scale upward motion would go up the equivalent potential temperature gradient, cooling the upper troposphere instead of warming it (Holton, 2004, pp. 371-372). The actual ascent in Earth's atmosphere occurs in localized cumulonimbus towers (Riehl & Malkus, 1958). Ascent in such "hot towers" is possible because a parcel beginning at the surface does in fact have a higher θ_e than the ambient air at any level between the surface and the tropopause, and thus will be positively buoyant during its entire ascent. On the other hand, for large-scale ascent to occur, the air initially at 600 hPa would also need to rise, and its θ_e is smaller than the overlying air.

The above discussion is valid for the annual-mean circulation. However, the meridional overturning circulation actually has a strong seasonal dependence. Since the Hadley cells are heat engines driven by the equator-to-pole gradient in net radiation, the amount of energy available to them depends on the strength of this gradient. Hence, while there are two Hadley cells at any given time, the one in the winter hemisphere is much stronger, due to the larger difference in net radiation in the winter hemisphere. The winter cell also encompasses a wider latitude band and involves cross-equatorial flow (James, 1994, p. 82; Holton, 2004, p. 324). Thus, the Northern Hemisphere cell dominates the circulation from November to March, the Southern Hemisphere cell dominates May to September, and there are fairly abrupt transitions between these two extreme states in April and October (Holton, 2004, p. 374).

On a non-rotating planet, the Hadley cells could extend from equator to pole in each hemisphere, and in fact, the Hadley cells on Venus, which rotates very slowly, do appear to reach much farther poleward than those on Earth—to about 45º latitude in each hemisphere (Ingersoll, 2013, p. 56). The effect of the Earth's rapid rotation, however, is to truncate the Hadley circulation. There are two separate reasons for this. (1) As the air in the upper-tropospheric branch of each cell moves poleward, it is deflected to the east by the Coriolis effect. As a consequence, the eastward velocity of the upper air creates a vertical wind shear which must satisfy the thermal wind relation.

For a very large poleward displacement of upper-tropospheric air, the wind shear would become too large for the meridional temperature gradient to balance it. At this point, the Hadley cell must terminate. The foregoing is essentially a conceptual summary of the Held and Hou model, (Held & Hou, 1980) and it shows that the Hadley circulation on a rotating planet must be meridionally limited even for a steady, zonally-symmetric flow. (2) In the real atmosphere, flow is not steady and zonally symmetric. Baroclinic instability develops in sufficiently large temperature gradients, which is likely what actually limits the meridional extent of the Hadley cells (Vallis et. al., 2015).

In addition to their role in energy transport, the Hadley cells dominate the spatial pattern of precipitation at low latitudes. The rising branch of this circulation occurs mostly in convection cells and is responsible for the intense precipitation in the Inter-Tropical Convergence Zone (ITCZ) and the tropical rainforests, and the sinking branches are responsible for the subtropical dry zones which contain many of the world's largest deserts. This pattern is especially apparent in Africa, where a nearly zonally symmetric pair of dry zones straddle an equatorial rain forest. The same pattern can be seen—although somewhat less cleanly—around the world. Southern Australia and the Atacama Desert are in the Southern Hemisphere dry zone; Mexico and the Arabian Peninsula are in the Northern Hemisphere dry zone; and the Amazon and Indonesia straddle the latitudes at which the ITCZ is normally found. Note, however, that some of these deserts are modified by other processes, including orographic effects and offshore ocean currents. The biggest interruption to this pattern is the Indian subcontinent and southeast Asia, which are much wetter than would be expected based on their latitude alone. Here the meridional temperature gradient is strongly modified on a seasonal basis by differential warming of the land and ocean surfaces, giving rise to a powerful monsoon circulation. Stated differently, the strong warming of the land in this region essentially moves the local thermal equator northward in boreal summer—and with it the ITCZ. In any case, the effect of the Hadley cells themselves can be more difficult to interpret in Asia, due to the more complex circulation in this region.

1.2 Expansion of the Hadley Cells

Climate models predict a meridional expansion of the Hadley cells as a result of global warming (Lu et. al., 2007; Gastineau et. al., 2008; Hu et. al., 2013; Vallis et. al., 2015). This possibility has attracted considerable interest, due to the expectation that any expansion of the Hadley circulation could cause a shift in the dry zones, and thus a significant change in the local water balance of certain regions (Scheff & Frierson, 2012; Feng & Fu, 2013). Since certain ecosystems are known to be very sensitive to changes in precipitation, (e.g. Hilker et. al., 2014) and since human societies are already over-exploiting water resources in many regions, (Ackerman and Stanton, 2011) any shift in the spatial pattern of precipitation is well worth investigating. Nonetheless, both the causes and effects of tropical expansion are still poorly understood.

Even for the modeled response of the Hadley cells to global warming, the mechanism is not entirely clear, though several hypotheses have been proposed. One hypothesis explains the Northern Hemisphere expansion in terms of an increase in the static stability of the subtropics (Lu et. al., 2007; Seo et. al., 2014). This would push the zone of baroclinic instability poleward, allowing the upper air to move farther poleward before sinking (Vallis et. al., 2015). A second hypothesis suggests that modeled expansion of the Hadley cells is due to an increase in the upper troposphere-lower stratosphere (UTLS) meridional temperature gradient due to faster warming in the tropical upper troposphere (Butler et. al., 2010; Gerber and Son, 2014). Whatever the mechanism, tropical expansion is a fairly robust effect of global warming: it occurs in most models and even an aqua planet model shows a similar response (Frierson et. al., 2007).

These modeling studies show how global warming could in principle drive Hadley cell expansion, but the observed expansion may also be responding to other drivers. In particular, many studies have found the observed expansion rate to be substantially larger than that indicated by the mean of global climate models over the historical period (Seidel et. al., 2008; Johanson & Fu, 2009; Hu et. al., 2013), suggesting either a deficiency in the models, an error in the reanalysis trends, or a large contribution from natural variability.

At least two separate questions are worth investigating here. First, what is driving the observed expansion of the Hadley cells? If the rapid expansion is in fact due to global warming—and if the reanalysis trends are accurate—then this would have important implications for any attempt to forecast the ecological and economic impacts, as it would mean that models have generally underestimated the sensitivity of this part of the climate system. On the other hand, if internal variability is driving most of the observed expansion, then the trend over the last several decades may not be representative of the long-term trend. In that case, the forcing due to global warming itself might be roughly as represented by the models.

Second, what effect does Hadley cell expansion have on subtropical and midlatitude precipitation? It is natural to expect that an expansion would cause drying on the poleward margins of the dry zones, but the strength and spatial pattern of this effect need to be quantified. Furthermore, it is not immediately clear to what degree the drying would be modified by zonally asymmetric processes, especially over land.

1.3 Causes of the Expansion

The potential discrepancy between the observed and modeled rates of expansion has led many authors to search for other possible drivers of Hadley cell expansion. Potential drivers could be anthropogenic, non-greenhouse gas (GHG) forcings, such as particulate matter, other forms of air pollution, or stratospheric ozone depletion; or they could be from natural forcings or internal variability. Both possibilities have been explored in the literature.

Several recent studies have suggested that global climate models can indeed capture the magnitude of the recent trends when natural variability is considered (Garfinkel et. al., 2015; Davis & Birner, 2017). In particular, the recent tropical expansion in the Northern Hemisphere (NH) may be largely explained by a trend in the Pacific Decadal Oscillation (PDO; Newman et. al., 2016) toward its cool phase (Allen et. al., 2014; Allen & Kovilakam, 2017).

However, anthropogenic, non-GHG forcing, such as increasing black carbon aerosols (Allen

et. al., 2012; Kovilakam & Mahajan, 2015), increasing tropospheric ozone (Allen et. al., 2012), and depletion of stratospheric ozone (Lu et. al., 2009; Son et. al., 2010; Polvani et. al., 2011; McLandress et. al., 2011; Waugh et. al., 2015) have also been proposed as contributors to the recent tropical expansion. Stratospheric ozone depletion, in particular, is a major driver of recent Southern Hemisphere (SH) climate change (Johanson and Fu, 2009; Lu et. al., 2009; Polvani et. al., 2011; Thompson et. al., 2011; Waugh et. al., 2015), making it unlikely that the recent expansion of the tropics in the SH can be explained by natural forcings alone.

To further complicate matters, it is not even clear that the recent widening is representative of a long-term trend. Other authors claim that the Hadley cells have overall been shrinking and intensifying since 1871, perhaps due to natural variability, with the reverse trend only in more recent decades (Liu et. al., 2012; Brönnimann et. al., 2015). However, the data available prior to 1979 is generally sparser, making expansion rates difficult to measure accurately.

In some sense, of course, the difficulty in attributing tropical expansion to a single cause is not surprising: climate forecasts—which often use a mean over many runs to represent forced variability only—are very often overwhelmed by internal variability in the short term (Deser, 2012; Kang et. al., 2013), and in this context, the "short term" can include the entire observed record since 1979.

In summary, while the link between global warming and Hadley cell expansion in models seems to be strong, the causes of observed Hadley cell expansion are not well understood. Possible drivers span the full range of natural variability, anthropogenic non-GHG forcing, and anthropogenic GHG forcing.

1.4 Zonal Asymmetry and the Effects of Tropical Expansion

Regardless of the causes, a second relevant question concerns the anticipated effects that Hadley cell expansion may have on spatial patterns of precipitation. Modeling studies have in fact found changes in precipitation resulting from expansion of the Hadley cells (Held and Soden, 2006;

Lau et. al., 2015; Rind and Perlwitz, 2004; Lu et. al., 2007; Kang & Polvani, 2011; Lau & Kim, 2015; Grise & Polvani, 2016) and there is some observational evidence that the dry zones have shifted and expanded (Cai, 2012; Feng and Fu, 2013; Fu, 2015; Zhou et. al., 2011), but a comparison of model runs with observations of rainfall changes suggests that the models have again underestimated the speed of the observed trends (Allan and Soden, 2007).

Several studies have begun to examine the recent Hadley cell expansion—and its effects—by longitude band. In general, these studies are consistent with the observation that interannual variability in the Hadley circulation is dominated by the Asia-Pacific sector where the largest tropical convective heat source is located (Nguyen et. al., 2017). For example, both Choi et. al. (2014) and Lucas and Nguyen (2015) attributed recent expansion to the Asia/Australia/Pacific sector.

The hydrological effects of Hadley cell expansion appear to be far from zonally symmetric. For example, semi-arid regions in southeast Australia have experienced drying trends in austral autumn that coincide with a poleward expansion of the Hadley circulation (Cai et. al., 2012; Cai & Cowan, 2013). However, drying trends in other semi-arid subtropical regions of the SH cannot as readily be explained by Hadley cell expansion (Cai et. al., 2012). Modeled drying trends also tend to show a contrast between land and oceans (Byrne and O'Gorman, 2015; He and Soden, 2016). While this study focuses on Hadley cell expansion and associated drying, it is important to note that subtropical precipitation also responds to several other processes, including thermodynamic effects (Seager et. al., 2010) and the direct radiative effects of CO_2 forcing (He and Soden, 2016). These processes are outside the scope of this study, but this is another reason to be cautious about any simple link between Hadley cell expansion and widespread subtropical drying.

The goal of this study is to document how Hadley cell width (defined by commonly used metrics of the zonal mean circulation) impacts the subtropical dry zones as a function of longitude. Our results reveal that traditional zonal-mean metrics of tropical expansion, such as the mean meridional streamfunction, emphasize circulation and precipitation changes over ocean basins, and

thus may be poor metrics for meridional shifts of precipitation over land.

2. Data and Methods

2.1 Observations

The observational data for this study are taken from a combination of in-situ, satellite-based, and reanalysis data products. For our primary observational data product, we use monthly-mean meridional wind and sea level pressure (SLP) from the European Centre for Medium-Range Weather Forecasts (ECMWF) Interim reanalysis data set (ERA-Interim; Dee et. al., 2011). We supplement the reanalysis data with monthly-mean precipitation from the Global Precipitation Climatology Project (GPCP; Adler et. al., 2003) and Climate Prediction Center Merged Analysis of Precipitation (CMAP; Xie &Arkin, 1997) data sets, which incorporate both ground-based and satellite estimates of precipitation. Unless otherwise noted, these data sets are analyzed over the period January 1979 to December 2015.

While reanalysis data are useful for many purposes, the trends in reanalysis variables can be biased by differences in the data sources assimilated in different parts of the time series (Kistler et. al., 2001; Sturaro, 2003). Thus, to calculate the SLP trend over the historical period (Fig. 1, top), we supplement the ERA-Interim data with monthly-mean SLP data from four additional reanalyses: 1) NCEP Climate Forecast System Reanalysis (CFSR; Saha et. al., 2010), 2) Japanese 55-year reanalysis (JRA-55; Kobayashi et. al., 2015), 3) NASA Modern-Era Retrospective analysis for Research and Application Version 2 (MERRA-2; Gelaro et. al., 2017), and 4) NCEP-DOE Reanalysis 2 (Kanamitsu et. al., 2002). We also examine gridded monthly SLP observations from the Hadley Centre SLP data set (HadSLP2r; Allan and Ansell, 2006), which relies solely on observations without the additional component of model forecasts. The common time period for all six data sets (five reanalyses and HadSLP2r) is January 1980 – December 2010. Over this period, in nearly all locations across the globe, at least five of the six data sets agree on the sign of the observed SLP trend (Fig. 1, top), and in most locations where the trend has large magnitude, all six

agree. Thus, while the exact magnitude of the recent observed SLP trend may be difficult to determine, the spatial pattern of the trend (which is the focus of this study) is quite consistent across data sets, giving us confidence in its robustness.

2.2 Models

The model data used in this study are the monthly-mean output from 15 global climate models that participated in phase 5 of the Coupled Model Intercomparison Project (CMIP5; Taylor et. al., 2012) (see list in Table 1). Runs from the following scenarios are examined: (1) sstClim, a 30-year-long scenario with unforced variability in which sea surface temperatures (SSTs) and sea ice are fixed to a seasonally varying control climatology; (2) historical, representing the climate model's response to observed natural and anthropogenic forcings over the period 1850–2005; (3) historicalGHG, same as the historical scenario but for greenhouse gas forcing only; and (4) historicalMisc, same as the historical scenario but for anthropogenic aerosol forcing only (labeled historicalAA in the figures). Very few CMIP5 models provide data for all of the desired scenarios, so we select the 15 models that have available data from at least three out of the four. For Figure 6, we also use (5) the piControl scenario, representing hundreds of years of preindustrial conditions (no anthropogenic forcings), and (6) the abrupt 4xCO_2 scenario, representing an abrupt quadrupling of carbon dioxide at the beginning of a 150-year-long run. For each scenario, we use only one ensemble member from each model, so that all models are weighted equally. Note, that while the abrupt 4xCO_2 runs include 150 years of data, we use only the last 50 years from these runs to approximate an equilibrated 4xCO_2 climate.

2.3 Methods

To quantify movement in the poleward boundary of the Hadley cells, we calculate monthly time series of the latitude at which the 500-hPa mean meridional streamfunction (Ψ_{500}) crosses zero poleward of its tropical extremum in each hemisphere. Note that the streamfunction at 500 hPa, as

a function of latitude ($\Psi_{500}(y)$) may be interpreted as the northward mass flux above the 500 hPa level. Hence, this function will be positive in the NH Hadley cell and negative in the NH Ferrell cell, and the reverse in the Southern Hemisphere. Hence, the latitude at which $\Psi_{500}(y) = 0$ in each hemisphere may be taken to be the poleward boundary of the hemispheric Hadley cell.

We compute the streamfunction using the zonal-mean meridional wind from ERA-Interim reanalysis or from the model data, as appropriate. We refer to these time series as Ψ_N for the NH and Ψ_S for the SH. We have verified that our results are not sensitive to our choice of the Ψ_{500} metric. Qualitatively similar results can be derived using time series of the latitude at which the zonal-mean zonal wind at the surface equals zero (not shown).

It is well known that the Hadley circulation expands during La Niña events and contracts during El Niño events (Lu et. al., 2008; Tandon et. al., 2012), so we also remove the El Niño-Southern Oscillation (ENSO) from the SLP and precipitation fields. To do this, we use the Niño 3.4 index time series provided courtesy of the NOAA Earth System Research Laboratory. This index is computed using the average of SSTs over the region: 5°N—5°S, 170—120°W, using monthly values of NOAA's Extended Reconstructed Sea Surface Temperature (ERSST) data set version 4. We then de-seasonalize and standardize this time series over the 1979—2015 period to yield a Niño 3.4 anomaly time series, which we denote as $N(t)$. We can then remove the effects of ENSO from an observed field $A(\boldsymbol{x}, t)$ as follows. At each location $\boldsymbol{x}$, let $R(\boldsymbol{x})$ be the slope of the linear regression of $A(\boldsymbol{x}, t)$ to $N(t)$. Then the ENSO-congruent time series at each location is $R(\boldsymbol{x})N(t)$, and the residual time series, after ENSO removal, is as follows:

$$B(\boldsymbol{x}, t) = A(\boldsymbol{x}, t) - R(\boldsymbol{x})N(t)$$

The ENSO removal is performed at lags of both -1 and 0 months, as the atmospheric teleconnections of ENSO often lag the tropical SSTs by several weeks (e.g., Alexander et. al., 2002).

3. Results

Figure 1 (top) shows the average observed trend in SLP over the period 1980–2010 from six observational data sets (see section 2.1). As discussed in the Introduction, previous studies have documented that the tropical belt is expanding in both hemispheres over this period, which should push the subtropical ridges and associated dry zones poleward (at least in a zonal mean sense). Note, however, that the recent trend in SLP—used here to track the movement of the subtropical ridge—is zonally asymmetric, particularly in the NH (Fig. 1, top). A key question then, is what portion of the observed SLP trend is attributable to the recent Hadley cell expansion.

To answer this question, we first need to understand how variability in the Hadley cell edge is manifested in the SLP field. Figure 2 (top row) shows the regression of ERA-Interim SLP onto the monthly time series of Ψ_N (left) and $-\Psi_S$ (right). Note that we have removed the trends and seasonal cycles from all fields prior to the regression analysis. The resulting regression patterns correspond to the SLP anomalies associated with a 1˚ poleward shift in the Hadley cell edge in each hemisphere. For reference, the positions of the climatological 1015 and 1020 hPa SLP contours are superimposed on the figure.

The results in Fig. 2 (top row) reveal that in both hemispheres, a poleward shift in the Hadley cell edge is associated with increased SLP in centers of action over midlatitude ocean basins, consistent with a poleward shift of the climatological anticyclones in those regions. However, the signature of a strengthened Walker circulation (La Niña) is also visible in these figures (positive SLP anomalies in the eastern tropical Pacific, negative SLP anomalies in the western tropical Pacific), consistent with the fact that La Niña events are associated with poleward shifts of the Hadley cell edge (e.g., Lu et. al., 2008). This raises an important question: do the patterns in Fig. 2 (top row) simply reproduce anomalies associated with ENSO?

To address this issue, we remove the effects of ENSO from the SLP field by subtracting the Niño 3.4-congruent component of SLP from each grid cell (as described in section 2.3), and then repeat the regression procedure used in Fig. 2 (top row). The results are shown in Fig. 2 (middle row). To verify that we removed ENSO correctly, we also show the regressions of SLP anomalies

on the Ψ_N and $-\Psi_S$ time series from the sstClim runs of CMIP5 models (Fig. 2, bottom row). Recall that the sstClim scenario prescribes climatological SSTs and sea ice and so, by definition, does not include ENSO or any other climate phenomena mediated by SST variability. The results for both the observations and models show that, while the tropical SLP response has been removed, the extratropical SLP response is essentially unchanged. Hence, the extratropical SLP response to variability in the Hadley cell extent is in fact zonally asymmetric and appears to be largely an atmospheric phenomenon, which can occur independently of coupled ocean-atmosphere dynamics. This result is consistent with the findings of previous studies, which have found a strong linkage between extratropical dynamics and variability in the Hadley cell extent (e.g., Kang et. al., 2013).

Figure 3 reproduces the results from Fig. 2, but with SLP replaced by precipitation. The precipitation anomalies associated with variability in Ψ_N and Ψ_S are much noisier than the SLP anomalies, and there are residual responses in the tropics even after ENSO is removed. Nonetheless, the same centers of action in the North Pacific, North Atlantic, and Southern Oceans can be discerned as in the SLP field (compare Figs. 2 and 3), particularly in the sstClim runs (Fig. 3, bottom row). These results illustrate that the zonal asymmetries identified in the SLP field are directly relevant for subtropical precipitation variability. In particular, drying occurs almost exclusively over oceans in the SH, and in the NH follows a zonally asymmetric pattern that favors the western sides of continents. Thus, the traditional view that Hadley cell expansion contributes to subtropical drying trends does not bear itself out over most subtropical land regions.

Having established the signature of Hadley cell expansion based on month-to-month variability, we now return to our original question concerning the role of Hadley cell expansion in recent trends of observed SLP and precipitation. The middle and bottom panels of Fig. 1 show the portion of the observed SLP trend that is congruent with changes in tropical width – measured in terms of Ψ_N and Ψ_S. Specifically, these two panels show the regression of SLP on Ψ_N and $-\Psi_S$ (as shown in Fig. 2, middle row), multiplied by the 1980-2010 trend in Ψ_N and $-\Psi_S$. Overall, the recent Hadley cell expansion can explain a large fraction of the SLP trends over the Southern Ocean

and a smaller fraction in the North Pacific basin, but the recent SLP trends over the North Atlantic basin are not consistent with Hadley cell expansion there. We choose not to examine observed precipitation trends (due to a lack of consistency among the two precipitation data sets), but the signature of Hadley cell expansion in recent regional precipitation trends can be qualitatively inferred from the patterns shown in Fig. 3.

One caveat to the analysis in Fig. 1 (middle and bottom) is that we have used month-to-month variability in Ψ_N and Ψ_S as a proxy for long-term variability. It is possible, however, that the short-term and long-term responses of SLP and precipitation to tropical widening may be very different (even after ENSO is removed). Thus, it is useful to compare the results in Fig. 1 with trends from the historical runs of CMIP5 models. Of course, this second approach comes with a caveat of its own—the trends in the historical runs also encompass changes in SLP and precipitation due to effects other than changes in the atmospheric general circulation—which is worth bearing in mind in the following discussion.

The top row of Figure 4 displays the multi-model-mean SLP and precipitation trends over the period 1980–2004 from the historical runs of CMIP5 models. The models' historical trends forced by greenhouse gas forcing only and anthropogenic aerosol forcing only are also shown in the middle and bottom rows of Fig. 4, respectively. Note that the historical and historical single forcing runs for many models end in 2004 or 2005, which requires us to truncate the trend calculation to the 1980–2004 period (as opposed to the 1980–2010 period used for the observations in Fig. 1, top). However, the observed trend over the period 1980-2004 (not shown) is nearly identical to the 1980-2010 trend (Fig. 1, top).

In the SH, the multi-model-mean historical SLP trends correspond very well with the observed trends shown in Fig. 1, showing a roughly zonally symmetric positive SLP trend at the poleward margins of the subtropics (Fig. 4, top left). The poleward expansion of the SH subtropical ridge is not only a characteristic of short-term variability in the Hadley cell edge latitude (Fig. 2) but is also a characteristic of the Hadley cell expansion driven by greenhouse gas forcing (Fig. 4,

middle; see also Fig. 6) and stratospheric ozone depletion (cf. Fig. 7 of Polvani et. al., 2011). Consequently, in the SH, the spatial pattern of SLP anomalies associated with Hadley cell expansion appears relatively independent of the underlying forcing. Note, however, that anthropogenic aerosols do not contribute to tropical expansion in the SH (Fig. 4, bottom left; see also Table 2).

In contrast, in the NH, the spatial pattern of SLP anomalies associated with Hadley cell expansion appears quite dependent on the underlying forcing. In the North Pacific, the multi-model-mean historical SLP trends are weakly positive and do not capture the large positive trends seen in observations (compare Fig. 4, top left with Fig. 1, top). Greenhouse gas forcing is associated with negative SLP trends over the North Pacific (Fig. 4, middle; see also Fig. 6), consistent with the fact that the North Pacific circulation does not shift robustly poleward in response to greenhouse gas forcing during most seasons (Scheff & Frierson, 2012; Grise and Polvani, 2014; Simpson et. al., 2014). Aerosol forcing is associated with a weak positive SLP trend over the 1980–2004 period (Fig. 4, bottom left), but the sign of the trend is not robust across models. Hence, the observed positive SLP trend over the North Pacific appears most consistent with year-to-year variability in the Hadley cell edge (Fig. 2), suggesting that natural variability might be its leading driver.

In the North Atlantic, the multi-model-mean historical SLP trends are weakly negative, but are of the same sign as those seen in observations (compare Fig. 4, top left with Fig. 1, top). Note that these negative SLP trends are in contrast to both the positive SLP anomalies associated with year-to-year variability (Fig. 2), and the positive SLP trends projected by models in response to greenhouse gas forcing (Fig. 4, middle; see also Fig. 6). Interestingly, the observed and historical model trends are consistent with anthropogenic aerosol forcing (Fig. 4, bottom left). Whether the observed negative SLP trends over the North Atlantic are driven by aerosol forcing (as the models suggest) or by natural variability uncorrelated with Ψ_N is a topic for future research.

Finally, we note that the regional precipitation trends projected by CMIP5 models over the

historical period (Fig. 4, right column) do not closely correspond with the precipitation anomalies associated with month-to-month variability in the Hadley cell edge (Fig. 3). The long-term trends in precipitation are complicated by the fact that precipitation also responds to thermodynamic factors (e.g., Seager et. al., 2010), and direct radiative effects of CO_2 forcing (He and Soden, 2016). It is perhaps unsurprising then, that the agreement among the models' long-term predictions and their month-to-month responses to Hadley cell width is better for SLP than for precipitation (compare left column of Fig. 4 with Fig. 2).

For Figure 4, we truncated the time series for consistency, which meant that the period over which we computed the trends was only 25 years—shorter than what we would normally prefer. Thus, to demonstrate that the pattern in Figure 4 is not merely the result of decadal variability, we show the trends for the same three historical scenarios, with the trend calculated over the full 1900-2004 period (Figure 5). Figures 4 and 5 have similar spatial patterns, suggesting that the pattern seen in Figure 4 is fairly robust. (Note, however, that the magnitude of the trends is much larger in Figure 4.)

Figures 4 and 5 (middle rows) demonstrate the response of SLP and precipitation to GHG forcing in a scenario representing observed historical increases in GHG concentrations, but this is not the only way to quantify GHG forcing. We could also consider a hypothetical scenario with a much larger—and abrupt—increase in GHG concentrations, followed by some time for the model to approximately equilibrate.

For Figure 6, we use two model scenarios in addition to those described in Section 2.3: (1) the piControl scenario, a control run representing hundreds of years of preindustrial conditions (i.e. with no anthropogenic forcings), and (2) the abrupt 4xCO2 scenario, which represents an abrupt quadrupling of CO_2 at the beginning of a 150-year run. We use only years 101 – 150 of the latter, in order to approximate an equilibrium climate response. The figure reports the difference between the resulting $4xCO_2$ climatology and the piControl climatology. Note the similarity of Figure 6 to the trends from the historicalGHG scenario in Figures 4 and 5 (middle row). The similarity

between Figure 6 and the middle rows of Figures 4 and 5 suggests that the transient climate response in the latter is similar to the approximate equilibrium climate response in the former.

4. Conclusions

In this study, we examine the degree to which the poleward expansion of the Hadley circulation (as measured from a zonal mean perspective) projects on regional SLP and precipitation patterns. From a zonal mean perspective, one might expect a poleward shift in the edge of the Hadley cells to be associated with a poleward shift in the subtropical ridge and associated dry zones at most longitudes. Here, we show that the SLP and precipitation anomalies associated with month-to-month variability in Hadley cell edge latitude are primarily zonally asymmetric, with preferred centers of action found over the oceans. Global climate models indicate that the longer-term trends in Hadley cell extent driven by anthropogenic forcing are also associated with similar centers of action over the oceans in the SLP field, whereas longer-term trends in the precipitation field are more strongly influenced by other factors.

Zonal mean circulation metrics (such as the Hadley circulation) provide a useful framework to quantify and understand the mechanisms behind recent and future changes in the atmospheric general circulation. However, the results of this study illustrate the limitations of such a zonal mean perspective. While poleward displacements of the Hadley circulation are associated with poleward shifts of the subtropical dry zones in the zonal mean, this is largely an oceanic signature and does not accurately describe surface changes over most land regions, especially in the NH. Consequently, to understand past and future precipitation changes driven by the atmospheric general circulation over land, a zonally asymmetric perspective is clearly warranted.

5. Future Work

5.1 Objective

My primary objective for future work is to determine the degree to which Hadley cell expansion drives drought and precipitation changes in North America on decadal to centennial timescales. The work described above took one step toward addressing this question by considering whether months with a wider Northern Hemisphere Hadley cell were also drier in certain locations, but this method addresses only *short-term* variability.

What this study does not show is how long-term (decadal to centennial) Hadley cell expansion might differ from the short-term (year-to-year) variability. The climate system includes coupled atmosphere-ocean processes operating on decadal and multi-decadal timescales—such as the Pacific Decadal Oscillation and Atlantic Multidecadal Oscillation (AMO; Schlesinger & Ramankutty, 1994)—as well as even longer-term trends due to climate change. There is no *a priori* guarantee that the patterns seen in Figure 1 will be representative of either the low-frequency variability or the trends. However, it is these low-frequency variabilities and trends that are most important for understanding climate changes in the 21st century and beyond.

To better understand the long-term response of precipitation and drought frequency to Hadley cell expansion, I will consider three primary questions:

1. Does Hadley cell expansion drive long-term drying trends in various regions of North America, and if so, which regions are most vulnerable?
2. Is Hadley cell expansion associated with an increase in the frequency of meteorological droughts?
3. What other dynamical processes in the climate system contribute to decadal variability and trends in precipitation?

5.2 Methodology

Station observations of precipitation over many Northern Hemisphere land regions are available over much of the 20th century, but the upper-tropospheric wind observations needed to

compute the Ψ_{500} metric are derived from satellite data and hence are only available for approximately the last 40 years. Consequently, the observational record is too short to examine decadal variability in Hadley cell extent, at least using this metric. To avoid this difficulty, I will use data from the Community Earth System Model Large Ensemble project (CESM-LENS; Kay et. al., 2015). This ensemble includes 40 runs of the CESM model from 1920 to 2100, using historical values of greenhouse gas concentrations and other forcings up to 2005, and the hypothetical Representative Concentration Pathway (RCP) 8.5 emissions scenario after 2005 (Meinshausen et. al., 2011). The 40 ensemble members use the same forcings but slightly different initial conditions—at the level of round-off error—in order to quantify the range of internal variability in the climate system.

These 40 historical runs will make it possible to address question (1) by comparing Hadley cell expansion rates and precipitation across ensemble members. I will then be able to determine whether members with more rapid Hadley cell expansion also have more rapid drying in certain regions of North America. Note, however, that while the 40 ensemble members have differing internal variabilities, they have identical forcings, so that any differences in Hadley cell expansion rates will be due to internal variability alone. Hence, while this approach will quantify the sensitivity of local precipitation to the variance in Hadley cell expansion rate, it will not address the sensitivity of local precipitation to the mean expansion rate. This distinction is potentially important, since the variance will be due to internal variabilities of the atmosphere-ocean system (potentially including the PDO and AMO) which may have different regional impacts than the mean expansion, which would be driven by the model's external forcing (including most importantly greenhouse gas trends).

I will also identify meteorological drought events in each model run, defined here as months in which total monthly precipitation at a particular location is at least 25% lower than the 20th century climatological mean from the same model run. I can then compare the frequency of droughts across North America in the second half of the 21st century using (a) the composite of the

10 model runs with the fastest Hadley cell expansion, and (b) the composite of the 10 runs with the slowest expansion, in order to address question (2).

CESM-LENS also includes three long control runs: a 2600-year atmosphere-only run (in which sea surface temperatures are fixed to a climatology), a 900-year slab ocean run (in which the atmosphere is coupled to the ocean but the ocean does not have any internal dynamics), and an 1800-year fully-coupled control run (with the atmosphere coupled to a fully dynamic, interactive ocean model), with preindustrial greenhouse gas concentrations in all three. I will use the first and third of these, and I will divide each into 30-year periods and consider the trends in precipitation and sea level pressure over each. Any such 30-year trends would be due to unforced variability, and depending on the control run used, this variability can include or exclude coupled atmosphere-ocean variability, such as El Niño and the Pacific Decadal Oscillation. Thus, I will be able to document the range of 30-year precipitation and sea level pressure trends over North America driven by internal atmosphere-only variability and coupled atmosphere-ocean variability, and contrast both with the trends found in the 21st century runs, in order to address question (3). I will also compare these model distributions with recent observed SLP trends, using the Hadley Centre SLP data set (HadSLP2r; Allan & Ansell, 2006) in order to determine how much recent trends depart from estimates of unforced variability.

5.3 Summary

In order to predict changes in North American precipitation and drought frequency over the 21st century, it will be crucial to understand the local effects of Hadley cell expansion. However, very little research has been done on this subject. This project would begin to fill that gap by identifying regions of North America that are most vulnerable to Hadley cell-induced drying, and quantifying the relative importance of forced Hadley cell expansion and internal variability.

Acknowledgments

Portions of this work were previously published in *Geophysical Research Letters* (Schmidt & Grise, 2017).

I would also like to thank my M.S. committee members—Kevin Grise, Bob Davis, and Todd Scanlon—for helpful discussions. This project was supported by start-up funding awarded to KMG by the University of Virginia. ERA-Interim data provided by ECMWF at http://apps.ecmwf.int/datasets. ERSST v4 data provided by NOAA CPC at http://www.cpc.ncep.noaa.gov/data/indices/. CMIP5 data provided by DOE/LLNL at http://esgf-node.llnl.gov/search/cmip5/. CFSR provided by NOAA-NCEI at https://www.ncdc.noaa.gov/data-access/model-data#cfsr. JRA-55 data provided by JMA at http://jra.kishou.go.jp/JRA-55/index_en.html. MERRA-2 data provided by NASA/GSFC at https://gmao.gsfc.nasa.gov/reanalysis/MERRA-2/. CMAP, GPCP, NCEP-DOE Reanalysis 2, and HadSLP2 data provided by the NOAA/OAR/ESRL PSD, Boulder, Colorado, at http://www.esrl.noaa.gov/psd/.

Figures

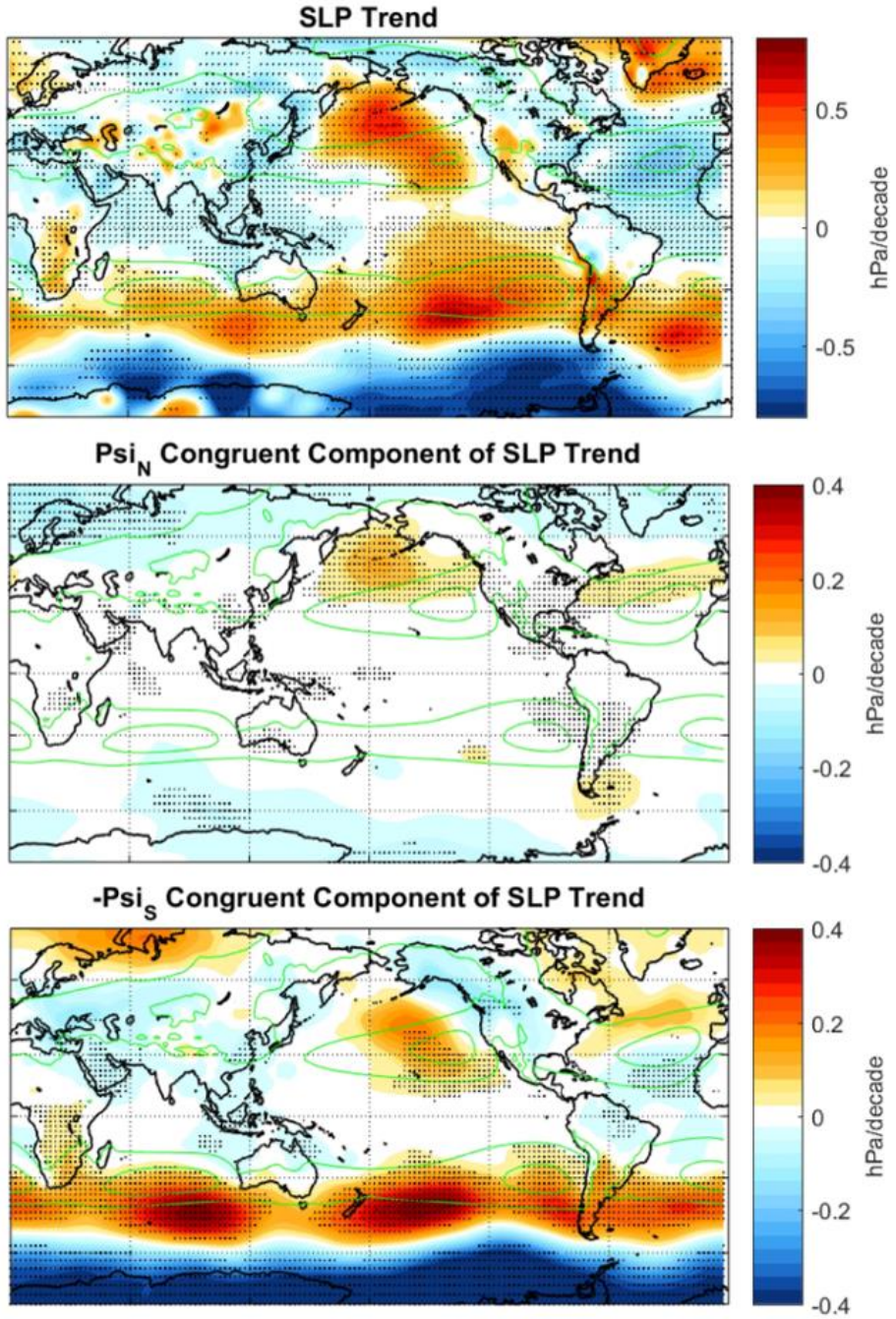

Figure 1. (top) SLP trend from 1980 to 2010, averaged over five reanalyses (CFSR, ERA-Interim, JRA-55, MERRA2, NCEP-DOE) and the Hadley Centre SLP data set. Stippling indicates that at least 5 out of 6 data sets agree on the sign of the trend. **(middle, bottom)** 1980–2010 ERA-Interim SLP trend congruent with the trends in the $\Psi_{500} = 0$ boundaries in each hemisphere, with ENSO removed (see section 2.3). Stippling indicates that the trend is statistically significant at the 0.95 level. Note the different color scale in the top panel. Climatological 1015 and 1020 hPa contours are in green.

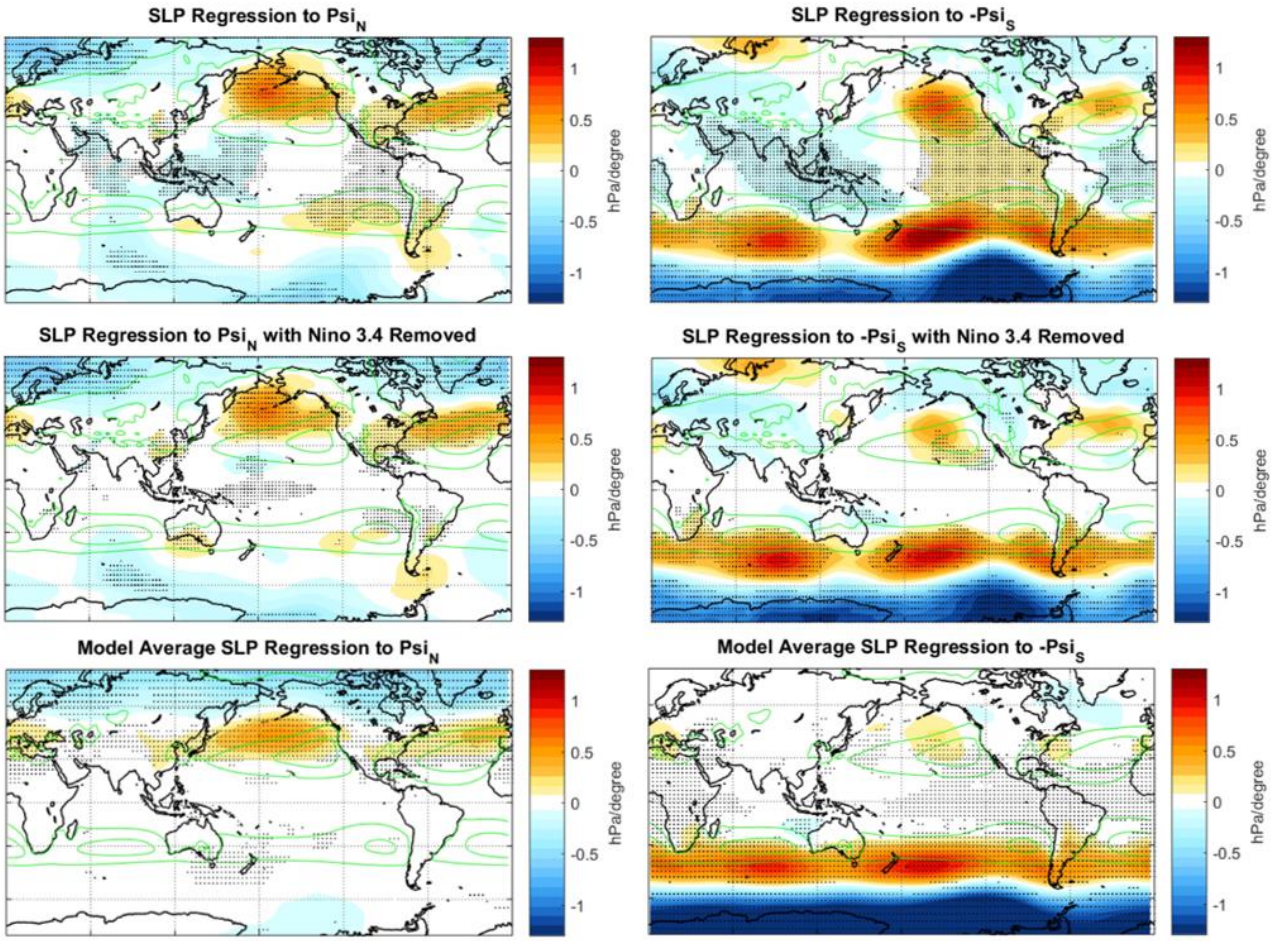

Figure 2. (top) Regression of monthly ERA-Interim SLP anomalies onto the Ψ_{500} = 0 boundaries in both hemispheres. **(middle)** As in top row, but with ENSO removed. **(bottom)** As in the top row, but using sstClim runs of CMIP5 models. Stippling indicates (top and middle rows) statistical significance at the 0.95 level, or (bottom row) agreement of at least 80% of models on the sign of the regression. Contours as in Figure 1. The regression patterns correspond to the SLP anomalies associated with a 1˚ poleward shift in the Hadley cell edge in each hemisphere.

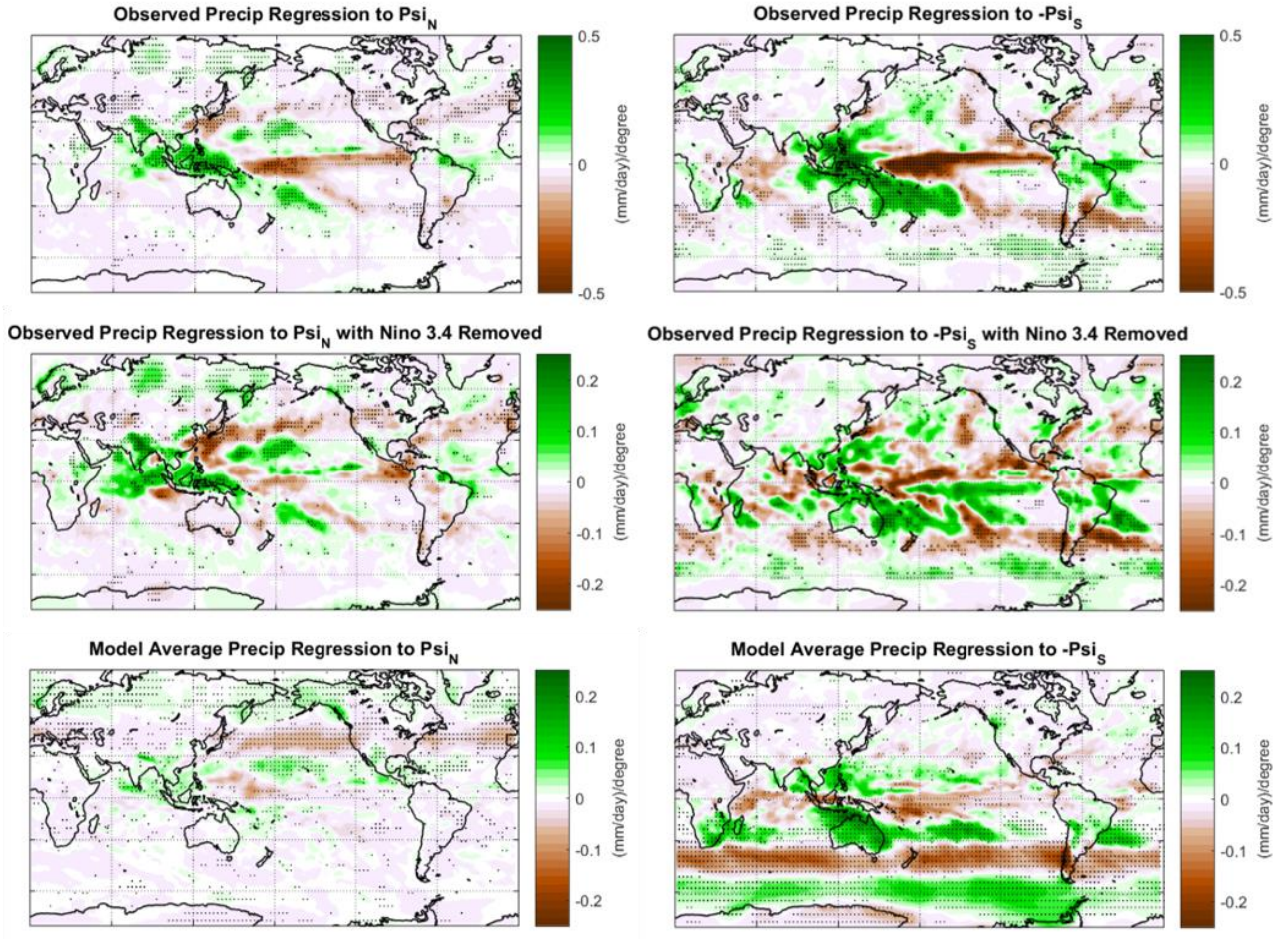

Figure 3. As in Fig. 2, but for regressions of monthly precipitation anomalies onto the $\Psi_{500} = 0$ boundaries. The top and middle rows show the average of the patterns from the GPCP and CMAP data sets. Note the different color scale in the top row.

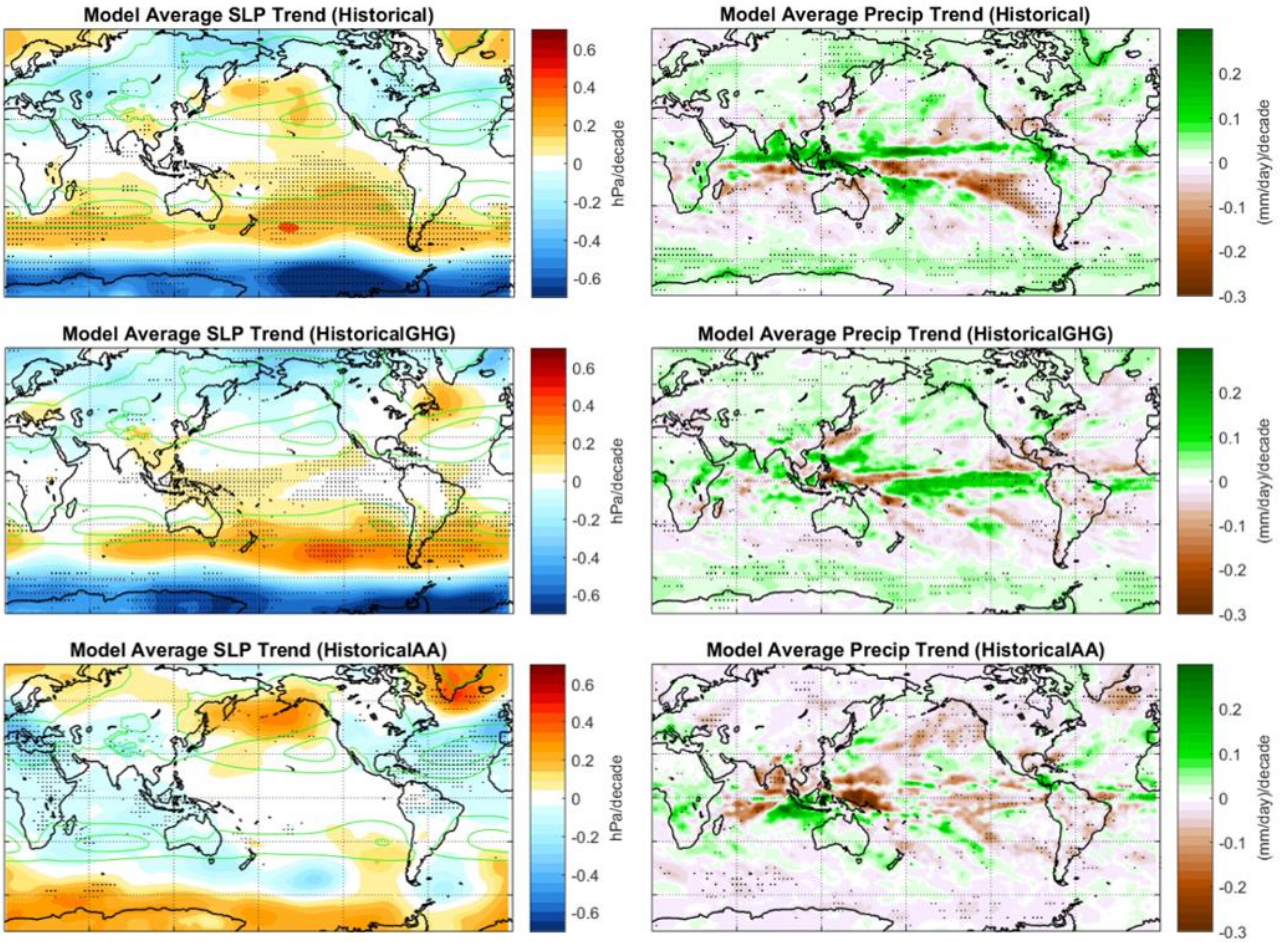

Figure 4. (top) Multi-model mean 1980-–2004 trends in the **(left)** SLP and **(right)** precipitation fields from the historical runs of CMIP5 models**. (middle)** As in the top row, but for the historicalGHG runs. **(bottom)** As in the top row, but for the historical aerosol-only runs. Stippling and contours as in Figure 2.

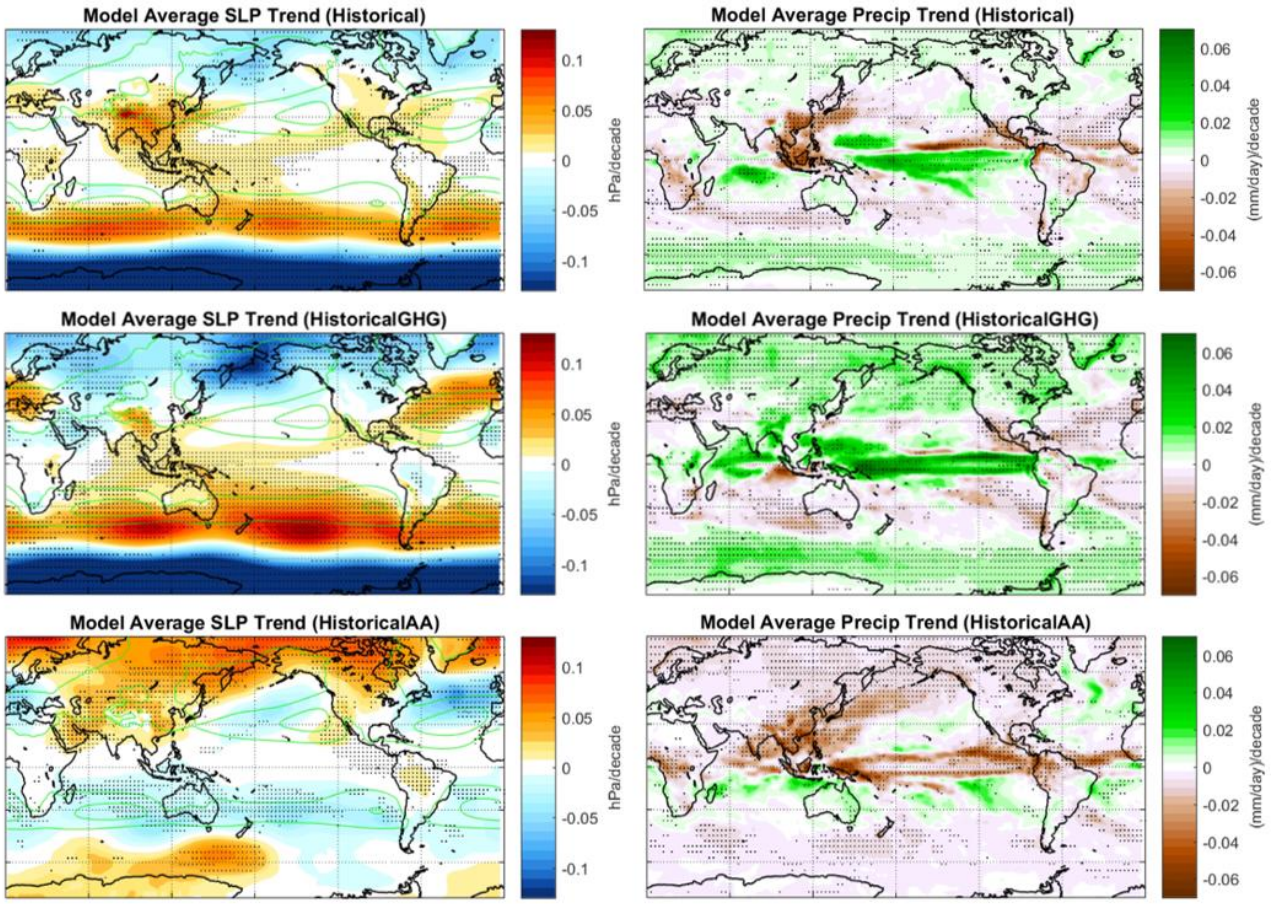

Figure 5. As in figure 4, but using the time period from January 1900 to December 2004.

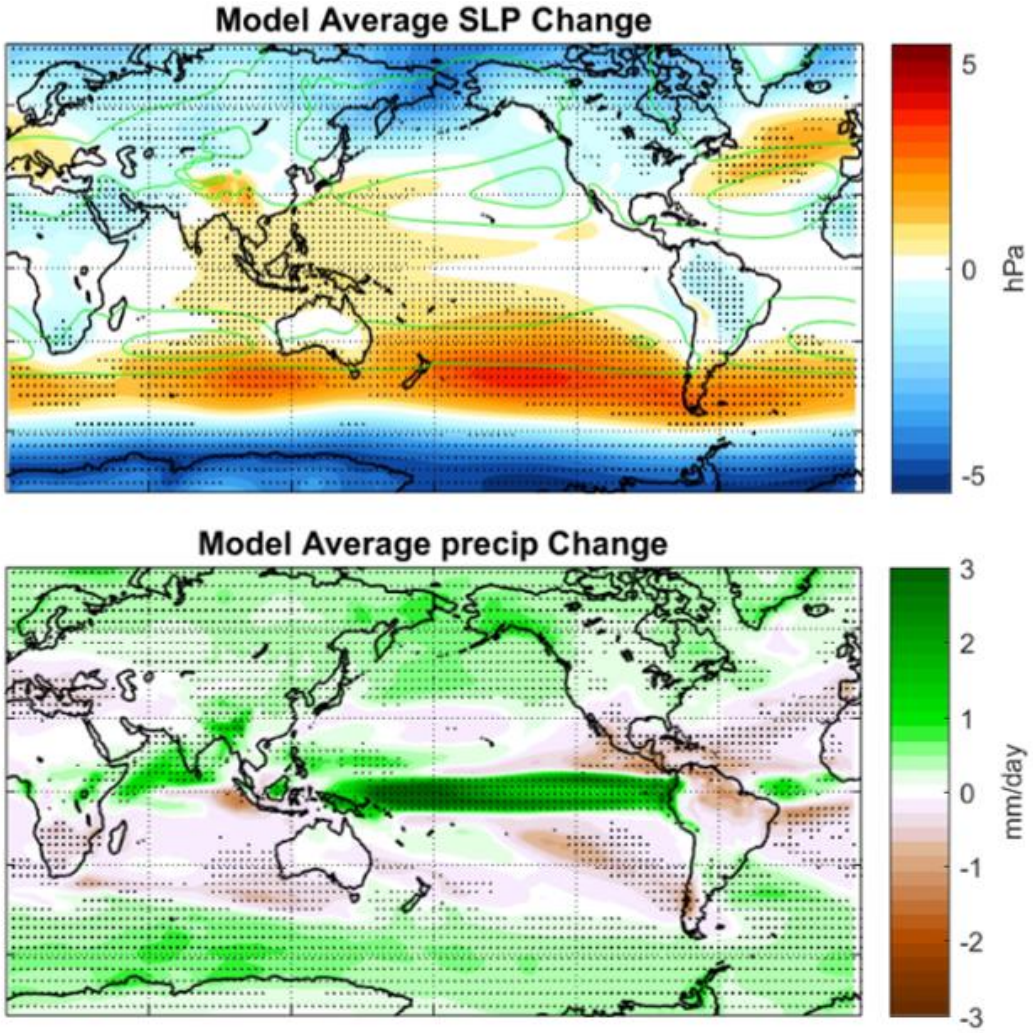

Figure 6. (top) Total change in sea-level pressure (SLP) from piControl to 4xCO2. Results are averaged over all of the 15 models listed in the table except CESM1-CAM5. Stippling indicates regions in which at least 80% of the models agree on the sign of the change. The total change is the difference between the time average for the last 50 years of the 4xCO2 run, and the time average for all years of the piControl run. **(bottom)** As above but showing the change in precipitation.

Model	Historical	Historical GHG	Historical Aerosol	sstClim
bcc-csm1-1	x	x		x
BNU-ESM	x	x		x
CanESM2	x	x	x	x
CCSM4	x	x	x	x
CESM1-CAM5	x	x	x	
CSIRO-Mk3-6-0	x	x	x	x
FGOALS-g2	x	x	x	
GFDL-CM3	x	x	x	x
GFDL-ESM2M	x	x	x	
GISS-E2-H	x	x	x	
GISS-E2-R	x	x	x	
HadGEM2-ES*	x	x		x
IPSL-CM5A-LR	x	x	x	x
MRI-CGCM3	x	x		x
NorESM1-M	x	x	x	x

*HadGEM2-A for sstClim

Table 1. List of the CMIP5 models used in the figures. X's indicate the availability of each run for the various models.

Average Psi trend (deg/decade)			
	historical	historicalGHG	historicalAA
NH	0.10	0.17	-0.04
SH	0.06	0.03	-0.05

Number of models with positive (poleward) trends			
	historical	historicalGHG	historicalAA
NH	11 out of 15	12 out of 15	7 out of 11
SH	10 out of 15	8 out of 15	1 out of 11

Table 2. (top) Trends in Hadley cell width calculated from historical and historical single-forcing models. **(bottom)** The number of individual models in each category with positive trends. Note that a positive trend represents a poleward motion, regardless of hemisphere.

References

Ackerman, F., & Stanton, E. A. (2011). The Last Drop: Climate Change and the Southwest Water Crises. Stockholm Environment Institute US. Retrieved from http://www.environmentportal.in/files/SEI-WesternWater-0211.pdf

Adler, R. F., Huffman, G. J., Chang, A., Ferraro, R., Xie, P.-P., Janowiak, J., … Nelkin, E. (2003), The Version-2 Global Precipitation Climatology Project (GPCP) Monthly Precipitation Analysis (1979–Present), *Journal of Hydrometeorology*, *4*(6), 1147–1167, doi:10.1175/1525-7541(2003)004<1147:TVGPCP>2.0.CO;2.

Alexander, M. A., Bladé, I., Newman, M., Lanzante, J. R., Lau, N.-C., & Scott, J. D. (2002), The Atmospheric Bridge: The Influence of ENSO Teleconnections on Air–Sea Interaction over the Global Oceans, *J. Climate*, *15*, 2205-2231.

Allan, R., & Ansell, T. (2006), A New Globally Complete Monthly Historical Gridded Mean Sea Level Pressure Dataset (HadSLP2): 1850–2004, *J. Climate*, 19, 5816-5842, doi:10.1175/JCLI3937.1.

Allen, R. J., & Kovilakam, M. (2017), The Role of Natural Climate Variability in Recent Tropical Expansion, *J. Climate*, doi:10.1175/JCLI-D-16-0735.1.

Allen, R. J., Norris, J. R., & Kovilakam, M. (2014), Influence of anthropogenic aerosols and the Pacific Decadal Oscillation on tropical belt width, *Nature Geosci.*, *7*(4), 270–274, doi:10.1038/ngeo2091.

Allen, R. J., Sherwood, S. C., Norris, J. R., & Zender, C. S. (2012), Recent Northern Hemisphere tropical expansion primarily driven by black carbon and tropospheric ozone, *Nature*, *485*(7398), 350–354, doi:10.1038/nature11097.

Birner, T. (2010), Recent widening of the tropical belt from global tropopause statistics: Sensitivities, *J. Geophys. Res.: Atmospheres*, *115*(D23), doi:10.1029/2010JD014664.

Birner, T., Davis, S. M., & Seidel, D. J. (2014), The changing width of Earth's tropical belt. *Physics Today, 67*(12), doi:10.1063/PT.3.2620.

Brönnimann, S., Fischer, A. M., Rozanov, E., Poli, P., Compo, G. P., & Sardeshmukh, P. D. (2015). Southward shift of the northern tropical belt from 1945 to 1980. *Nature Geosci.*, 8(12), 969–974, doi:10.1038/ngeo2568

Butler, A. H., Thompson, D. W. J., & Heikes, R. (2010). The Steady-State Atmospheric Circulation Response to Climate Change–like Thermal Forcings in a Simple General Circulation Model. *J. Climate*, 23(13), 3474–3496, doi:10.1175/2010JCLI3228.1

Byrne, M. P. & O'Gorman, P. A. (2015), The Response of Precipitation Minus Evapotranspiration to Climate Warming: Why the "Wet-Get-Wetter, Dry-Get-Drier" Scaling Does Not Hold over Land. *J. Climate*, 28, 8078–8092, doi:10.1175/JCLI-D-15-0369.1.

Cai, W., & Cowan, T. (2013), Southeast Australia Autumn Rainfall Reduction: A Climate-Change-Induced Poleward Shift of Ocean–Atmosphere Circulation, *J. Climate*, 26, 189-205, doi:10.1175/JCLI-D-12-00035.1.

Cai, W., Cowan, T., & Thatcher, M. (2012), Rainfall reductions over Southern Hemisphere semi-arid regions: the role of subtropical dry zone expansion, *Sci. Rep.*, *2*, article number 702, doi:10.1038/srep00702.

Chen, S., Wei, K., Chen, W., & Song, L. (2014). Regional changes in the annual mean Hadley circulation in recent decades. *J. Geophys. Res.: Atmospheres*, 119(13), 7815–7832, doi:10.1002/2014JD021540

Chiew, F. H. S., Piechota, T. C., Dracup, J. A., & McMahon, T. A. (1998). El Nino/Southern Oscillation and Australian rainfall, streamflow and drought: Links and potential for forecasting. *Journal of Hydrology*, 204(1), 138–149, doi:10.1016/S0022-1694(97)00121-2

Choi, J., Son, S.-W., Lu, J., & Min, S.-K. (2014), Further observational evidence of Hadley cell widening in the Southern Hemisphere, *Geophys. Res. Lett.*, *41*(7), 2590–2597, doi:10.1002/2014GL059426.

Davis, N., & Birner, T. (2017), On the Discrepancies in Tropical Belt Expansion between Reanalyses and Climate Models and among Tropical Belt Width Metrics, *J. Climate*, *30*(4), 1211–1231, doi:10.1175/JCLI-D-16-0371.1.

Davis, S. M., & Rosenlof, K. H. (2012), A Multidiagnostic Intercomparison of Tropical-Width Time Series Using Reanalyses and Satellite Observations, *J. Climate*, 25, 1061-1078, doi:10.1175/JCLI-D-11-00127.1.

Dee, D. P., Uppala, S. M., Simmons, A. J., Berrisford, P., Poli, P., Kobayashi, S., … Vitart, F. (2011), The ERA-Interim reanalysis: configuration and performance of the data assimilation system, *Quarterly Journal of the Royal Meteorological Society*, *137*(656), 553–597, doi:10.1002/qj.828.

Deser, C., Knutti, R., Solomon, S., & Phillips, A. S. (2012). Communication of the role of natural variability in future North American climate. *Nature Climate Change*, 2(11), 775–779, doi:10.1038/nclimate1562

Ding, Q., Steig, E. J., Battisti, D. S., & Wallace, J. M. (2012). Influence of the Tropics on the Southern Annular Mode. *J. Climate*, 25(18), 6330–6348, doi:10.1175/JCLI-D-11-00523.1

Feng, S., & Fu, Q. (2013), Expansion of global drylands under a warming climate. *Atmos. Chem. Phys.*, *13*(19), 10081–10094, doi:10.5194/acp-13-10081-2013.

Frierson, D. M. W., Lu, J. & Chen, G. (2007), Width of the Hadley cell in simple and comprehensive general circulation models. *Geophys. Res. Lett*., *34*, L18804, doi:10.1029/2007GL031115.

Fu, Q., Johanson, C. M., Wallace, J. M., & Reichler, T. (2006), Enhanced Mid-Latitude Tropospheric Warming in Satellite Measurements, *Science*, *312*(5777), 1179–1179, doi:10.1126/science.1125566.

Garfinkel, C. I., Waugh, D. W., & Polvani, L. M. (2015), Recent Hadley cell expansion: The role of internal atmospheric variability in reconciling modeled and observed trends, *Geophys. Res. Lett.*, *42*(24), doi:10.1002/2015GL066942.

Gastineau, G., Le Treut, H., & Li, L. (2008), Hadley circulation changes under global warming conditions indicated by coupled climate models, *Tellus A*, *60*(5), 863–884, doi:10.1111/j.1600-0870.2008.00344.x.

Gelaro, R., McCarty, W., Suárez, M. J., Todling, R., Molod, A., Takacs, L., … Zhao, B. (2017), The Modern-Era Retrospective Analysis for Research and Applications, Version 2 (MERRA-2), *J. Climate*, 30, 5419–5454, doi:10.1175/JCLI-D-16-0758.1.

Gerber, E. P., & Son, S.-W. (2014). Quantifying the Summertime Response of the Austral Jet Stream and Hadley Cell to Stratospheric Ozone and Greenhouse Gases. *J. Climate*, 27(14), 5538–5559, doi:10.1175/JCLI-D-13-00539.1

Grise, K. M., & Polvani, L. M. (2014), The response of midlatitude jets to increased CO2: Distinguishing the roles of sea surface temperature and direct radiative forcing, *Geophys. Res. Lett.*, *41*(19), 6863–6871, doi:10.1002/2014GL061638.

Grise, K. M., & Polvani, L. M. (2016), Is climate sensitivity related to dynamical sensitivity? *J. Geophys. Res.: Atmospheres*, *121*(10), 5159–5176, doi:10.1002/2015JD024687.

He, J., & Soden, B. (2016), A re-examination of the projected subtropical precipitation decline, *Nature Climate Change*, *7*, doi:10.1038/nclimate3157.

Held, I. M. & Hou, A. Y. (1980). Nonlinear Axially Symmetric Circulations in a Nearly Inviscid Atmosphere. *Journal of the Atmospheric Sciences*, *37*, 515–533, doi:10.1175/1520-0469(1980)037<0515:NASCIA>2.0.CO;2

Held, I. M., & Soden, B. J. (2006). Robust responses of the hydrological cycle to global warming. *J. Climate*, 19(21), 5686–5699, doi:10.1175/JCLI3990.1

Hendon, H. H., Lim, E.-P., & Nguyen, H. (2014). Seasonal Variations of Subtropical Precipitation Associated with the Southern Annular Mode. *J. Climate*, 27(9), 3446–3460, doi:10.1175/JCLI-D-13-00550.1

Hilker, T., Lyapustin, A. I., Tucker, C. J., Hall, F. G., Myneni, R. B., Wang, Y., … Sellers, P. J. (2014). Vegetation dynamics and rainfall sensitivity of the Amazon. *Proceedings of the*

National Academy of Sciences, 111(45), 16041–16046.

Holton, J. (2004). An Introduction to Dynamic Meteorology, Fourth Edition. New York. Elsevier Academic Press.

Hu, Y., & Fu, Q. (2007), Observed poleward expansion of the Hadley circulation since 1979, *Atmospheric Chemistry and Physics*, *7*(19), 5229–5236.

Hu, Y., Tao, L., & Liu, J. (2013), Poleward expansion of the hadley circulation in CMIP5 simulations. *Advances in Atmospheric Sciences*, *30*, 790–795, doi:10.1007/s00376-012-2187-4.

Ingersoll, A. (2013). Planetary Climates. New York. Princeton, New Jersey. Princeton University Press.

James, I. (1994). Introduction to Circulating Atmospheres. New York. Cambridge University Press.

Johanson, C. M., & Fu, Q. (2009), Hadley Cell Widening: Model Simulations versus Observations. *J. Climate*, *22*(10), 2713–2725, doi:10.1175/2008JCLI2620.1.

Kanamitsu, M., Ebisuzaki, W., Woollen, J., Yang, S.-K., Hnilo, J. J., Fiorino, M., & Potter, G. L. (2002), NCEP–DOE AMIP-II Reanalysis (R-2), *Bull. Amer. Meteor. Soc.,* 83, 1631–1643, doi:10.1175/BAMS-83-11-1631.

Kang, S. M., Deser, C., & Polvani, L. M. (2013), Uncertainty in Climate Change Projections of the Hadley Circulation: The Role of Internal Variability, *J. Climate*, *26*(19), 7541–7554, doi:10.1175/JCLI-D-12-00788.1.

Kang, S. M., & Polvani, L. M. (2011), The Interannual Relationship between the Latitude of the Eddy-Driven Jet and the Edge of the Hadley Cell, *J. Climate,* 24, 563–568, doi:10.1175/2010JCLI4077.1.

Kay, J. E., Deser, C., Phillips, A., Mai, A., Hannay, C., Strand, G., … Vertenstein (2015), The Community Earth System Model (CESM) Large Ensemble Project: A Community Resource for Studying Climate Change in the Presence of Internal Climate Variability, *Bull. Amer.*

Meteor. Soc., *96*, 1333–1349, https://doi.org/10.1175/BAMS-D-13-00255.1

Kistler, R., Kalnay, E., Collins, W., Saha, S., White, G., Woollen, J., … Kanamitsu, M. (2001), The NCEP–NCAR 50-Year Reanalysis: Monthly means CD-ROM and documentation. Presented at the Bull. Amer. Meteor. Soc.

Kobayashi, S., Ota, Y., Harada, Y., Ebita, A., Moriya, M., Onoda, H., … Takahashi, K. (2015), The JRA-55 Reanalysis: General Specifications and Basic Characteristics, *Journal of the Meteorological Society of Japan. Ser. II*, *93*(1), 5–48, doi:10.2151/jmsj.2015-001.

Kovilakam, M., & Mahajan, S. (2015), Black carbon aerosol-induced Northern Hemisphere tropical expansion, *Geophys. Res. Lett.*, *42*(12), 4964–4972, doi:10.1002/2015GL064559.

Lau, W. K. M., & Kim, K.-M. (2015), Robust Hadley Circulation changes and increasing global dryness due to CO2 warming from CMIP5 model projections, *Proceedings of the National Academy of Sciences*, *112*(12), 3630–3635, doi:10.1073/pnas.1418682112.

Liu, J., Song, M., Hu, Y., & Ren, X. (2012). Changes in the strength and width of the Hadley Circulation since 1871. *Climate of the Past*, 8(4), 1169–1175, doi:10.5194/cp-8-1169-2012

Lu, J., Chen, G., & Frierson, D. M. W. (2008). Response of the Zonal Mean Atmospheric Circulation to El Niño versus Global Warming. *J. Climate*, 21(22), 5835–5851, doi:10.1175/2008JCLI2200.1

Lu, J., Chen, G., & Frierson, D. M. W. (2008), Response of the Zonal Mean Atmospheric Circulation to El Niño versus Global Warming, *J. Climate*, *21*(22), 5835–5851, doi:10.1175/2008JCLI2200.1.

Lu, J., Deser, C., & Reichler, T. (2009), Cause of the widening of the tropical belt since 1958, *Geophys. Res. Lett.*, *36*(3), L03803, doi:10.1029/2008GL036076.

Lu, J., Vecchi, G. A., & Reichler, T. (2007), Expansion of the Hadley cell under global warming, *Geophys. Res. Lett.*, *34*(6), doi:10.1029/2006GL028443.

Lucas, C., & Nguyen, H. (2015), Regional characteristics of tropical expansion and the role of climate variability, *J. Geophys. Res.: Atmospheres*, *120*(14), 6809–6824,

doi:10.1002/2015JD023130.

Lucas, C., Timbal, B., & Nguyen, H. (2014), The expanding tropics: a critical assessment of the observational and modeling studies, *Wiley Interdisciplinary Reviews: Climate Change*, *5*(1), 89–112, doi:10.1002/wcc.251.

McLandress, C., Shepherd, T. G., Scinocca, J. F., Plummer, D. A., Sigmond, M., Jonsson, A. I., & Reader, M. C. (2011), Separating the Dynamical Effects of Climate Change and Ozone Depletion. Part II: Southern Hemisphere Troposphere, *J. Climate,* 24, 1850–1868, doi:10.1175/2010JCLI3958.1.

Meinshausen, M., Smith, S.J., Calvin, K. V., Daniel, J. S., Kainuma, M., Lamarque, J.-F., ... van Vuuren, D. (2011), The RCP Greenhouse Gas Concentrations and their Extension from 1765 to 2300, *Climate Change*, *109*, 213-241.

Newman, M., Alexander, M. A., Ault, T. R., Cobb, K. M., Deser, C., Di Lorenzo, E., … Smith, C. A. (2016), The Pacific Decadal Oscillation, Revisited, *J. Climate*, *29*, 4399–4427, doi:10.1175/JCLI-D-15-0508.1

Nguyen, H., Hendon, H. H., Lim, E.-P., Boschat, G., Maloney, E., & Timbal, B. (2017), Variability of the extent of the Hadley circulation in the southern hemisphere: a regional perspective, *Climate Dynamics*, 1–14, doi:10.1007/s00382-017-3592-2.

Polvani, L. M., Waugh, D. W., Correa, G. J. P., & Son, S.-W. (2011), Stratospheric Ozone Depletion: The Main Driver of Twentieth-Century Atmospheric Circulation Changes in the Southern Hemisphere, *J. Climate,* 24, 795–812, doi:10.1175/2010JCLI3772.1.

Riehl, H. & Malkus, J. (1958), On the heat balance in the equatorial trough zone, *Geophysica*, 6, 503-538.

Rikus, L. (2015), A simple climatology of westerly jet streams in global reanalysis datasets part 1: mid-latitude upper tropospheric jets, *Clim. Dyn.,* doi:10.1007/s00382-015-2560-y.

Rind, D., and Perlwitz, J. (2004). The response of the Hadley circulation to climate changes, past and future. In The Hadley Circulation: Past, Present and Future. H. F. Diaz, and R. S.

Bradley, Eds., Advances in Global Climate Change Research, volume 21. Springer Verlag, 399-435.

Saha, S., Moorthi, S., Pan, H.-L., Wu, X., Wang, J., Nadiga, S., … Goldberg, M. (2010), The NCEP Climate Forecast System Reanalysis, *Bull. Amer. Meteor. Soc.,* 91, 1015–1057, doi:10.1175/2010BAMS3001.1.

Scheff, J., & Frierson, D. M. W. (2012), Robust future precipitation declines in CMIP5 largely reflect the poleward expansion of model subtropical dry zones, *Geophys. Res. Lett.*, *39*(18), doi:10.1029/2012GL052910.

Schlesinger, M. E., & Ramankutty, N. (1994), An oscillation in the global climate system of period 65-70 years, *Nature*, *367*, 723–726, doi:10.1038/367723a0.

Schmidt, D. F., & Grise, K. M. (2017). The response of local precipitation and sea level pressure to Hadley cell expansion. Geophysical Research Letters, 44, 10,573–10,582, doi:10.1002/2017GL075380.

Seager, R., Naik, N., Vecchi, G. A. (2010), Thermodynamic and Dynamic Mechanisms for Large-Scale Changes in the Hydrological Cycle in Response to Global Warming, *J. Climate,* 23, 4651–4668, doi:10.1175/2010JCLI3655.1.

Seidel, D. J., Fu, Q., Randel, W. J., & Reichler, T. J. (2008), Widening of the tropical belt in a changing climate, *Nature Geosci.*, *1*(1), 21–24, doi:10.1038/ngeo.2007.38.

Seidel, D. J., & Randel, W. J. (2007), Recent widening of the tropical belt: Evidence from tropopause observations, *J. Geophys. Res.*, *112*(D20), doi:10.1029/2007JD008861.

Simpson, I. R., Shaw, T. A., & Seager, R. (2014), A Diagnosis of the Seasonally and Longitudinally Varying Midlatitude Circulation Response to Global Warming, *Journal of the Atmopheric Sciences,* 71, 2489–2515, doi:10.1175/JAS-D-13-0325.1.

Solomon, A., Polvani, L. M., Waugh, D. W., Davis, S. M. (2016), Contrasting upper and lower atmospheric metrics of tropical expansion in the Southern Hemisphere, *Geophys. Res. Letters*, *43*(19), doi: 10.1002/2016GL070917.

Seo, K.-H., Frierson, D. M. W., & Son, J.-H. (2014). A mechanism for future changes in Hadley circulation strength in CMIP5 climate change simulations. *Geophys. Res. Letters*, 41(14), 2014GL060868, doi:10.1002/2014GL060868

Son, S.-W., Gerber, E. P., Perlwitz, J., Polvani, L. M., Gillett, N. P., Seo, K.-H., … Yamashita, Y. (2010), Impact of stratospheric ozone on Southern Hemisphere circulation change: A multimodel assessment, *J. Geophys. Res.: Atmospheres*, *115*(D3), doi:10.1029/2010JD014271.

Sturaro, G. (2003), A closer look at the climatological discontinuities present in the NCEP/NCAR reanalysis temperature due to the introduction of satellite data, *Climate Dynamics*, *21*(3–4), 309–316, doi:10.1007/s00382-003-0334-4.

Tandon, N. F., Gerber, E. P., Sobel, A. H., & Polvani, L. M. (2012), Understanding Hadley Cell Expansion versus Contraction: Insights from Simplified Models and Implications for Recent Observations, *J. Climate*, *26*(12), 4304–4321, doi:10.1175/JCLI-D-12-00598.1.

Taylor, K. E., Stouffer, R. J., & Meehl, G. A. (2012), An Overview of CMIP5 and the Experiment Design, *Bull. Amer. Meteor. Soc.*, 93, 485–498, doi:10.1175/BAMS-D-11-00094.1.

Thompson, D. W. J., Solomon, S., Kushner, P. J., England, M. H., Grise, K. M., & Karoly, D. J. (2011), Signatures of the Antarctic ozone hole in Southern Hemisphere surface climate change, *Nature Geosci.*, *4*, 741–749.

Vallis, G. K., Zurita-Gotor, P., Cairns, C., & Kidston, J. (2015), Response of the large-scale structure of the atmosphere to global warming: Response of Atmospheric Structure to Global Warming, *Quarterly Journal of the Royal Meteorological Society*, *141*(690), 1479–1501, doi:10.1002/qj.2456.

Waugh, D. W., Garfinkel, C. I., & Polvani, L. M. (2015), Drivers of the Recent Tropical Expansion in the Southern Hemisphere: Changing SSTs or Ozone Depletion? *J. Climate*, *28*(16), 6581–6586, doi:10.1175/JCLI-D-15-0138.1.

Xie, P., & Arkin, P. A. (1997), Global Precipitation: A 17-Year Monthly Analysis Based on Gauge

Observations, Satellite Estimates, and Numerical Model Outputs, *Bull. Amer. Meteor. Soc.*, *78*(11), 2539–2558, doi:10.1175/1520-0477(1997)078<2539:GPAYMA>2.0.CO;2.

Zhang, M., & Song, H. (2006). Evidence of deceleration of atmospheric vertical overturning circulation over the tropical Pacific. *Geophys. Res. Letters*, 33(12), doi:10.1029/2006GL025942

Zhou, Y. P., Xu, K.-M., Sud, Y. C., & Betts, A. K. (2011). Recent trends of the tropical hydrological cycle inferred from Global Precipitation Climatology Project and International Satellite Cloud Climatology Project data. *J. Geophys. Res.: Atmospheres*, 116(D9), D09101, doi:10.1029/2010JD015197